Magnetic properties of $R_6Fe_{13-x}M_{1+x}$ compounds and their hydrides

C. H. de Groot, K. H. J. Buschow, and F. R. de Boer

Van der Waals-Zeeman Institute, University of Amsterdam, Valckenierstraat 65, 1018 XE Amsterdam, The Netherlands

The magnetic properties of various $R_6Fe_{13-x}M_{1+x}$ compounds (R=La, Nd, Gd, and Dy) crystallizing in the $La_6Co_{11}Ga_3$ structure have been investigated by magnetic measurements and x-ray diffraction. It is shown that all $Nd_6Fe_{13}M$ compounds with M=Au, Ag, Cu, Si, and Ga order antiferromagnetically around 415 K and evidence is provided that the frequently reported, increase of the magnetization at lower temperature is due to impurities. High-field measurements made at 4.2 K on $Nd_{6-x}Dy_xFe_{12.7}Ga_{1.3}$ compounds with x=0.0, 0.2, 0.5, and 1.0 show that the R-Fe coupling is not yet broken at 35 T. A large hysteresis in the field dependence of the magnetization is present in all compounds including $La_6Fe_{11}Al_3$, indicating the role of the Fe-sublattice anisotropy. A theoretical model for the field dependence of the magnetization is constructed, based on local minimization of the free energy. By taking into account the second- and fourth-order magnetocrystalline anisotropy terms, the magnetization behavior of the compounds, including the large hysteresis, can be explained excellently. A structure of ferromagnetically ordered Fe sheets coupling antiferromagnetically to each other is proposed to explain the experimental data. The hydrides of these compounds are all ferromagnetic (light R) or ferrimagnetic (heavy R) and have an easy magnetization direction along the c axis due to the Fe-sublattice anisotropy. Their ordering temperatures are near 450 K, just slightly above the Néel temperature of the parent compounds, which can be understood from the proposed spin structure.
[S0163-1829(98)09617-9]

I. INTRODUCTION

The crystal structure of the $R_6Fe_{13-x}M_{1+x}$ compounds (R=rare earth) was unraveled in 1985 by Sichevich *et al.*[1] They have shown that $La_6Co_{11}Ga_3$ orders in a tetragonal structure with space group $I4/mcm$. Later, Allemand *et al.*[2] have shown that $Nd_6Fe_{13}Si$ crystallizes as an ordered variant of this compound. Both structure types are interesting from a technological point of view since their presence as second phase in NdFeB-permanent magnets enhances the coercivity.[3] The crystallographic structure is complicated with four different Fe sites and two Nd sites. The R atoms (especially those at the $16l$ site) have mainly other R atoms as nearest neighbors. This has induced speculations that in these compounds the $4f$-$4f$ interaction, which is normally much smaller than the $4f$-$3d$ and $3d$-$3d$ interaction, might be of importance.[4]

A strong debate about the magnetic behavior of the ordered variant has arisen. Claims about ferromagnetism,[5] ferromagnetism with compensation point,[6] and antiferromagnetism[2,7,8] have been made. This controversion has prompted us to prepare the compounds $Nd_6Fe_{13}M$ with M=Au, Ag, Cu, and Si single phase as far as possible and to reexamine their magnetic behavior.

Another point of discussion is the spin configuration at the different sites. Heuristic reasoning[9–11] and neutron-diffraction experiments[6] have led to various configurations. By introducing a small amount of Dy (the $R_6Fe_{13}M$ structure is not stable for heavy-R elements[9]) in the compound $Nd_6Fe_{12.7}Ga_{1.3}$, we are able to obtain more information on the spin configuration of the R moments and their coupling to the Fe moments.

Coey *et al.*[4] have shown that all $R_6Fe_{13}M$ compounds ab-

sorb large amounts of hydrogen without any change in symmetry. From Mössbauer-effect experiments, they derive values of the Fe moment, which are incompatible with magnetization measurements when full ferromagnetic alignment of the moments is assumed. Hydrogenation of the Dy-substituted compounds leads to important information on the R-Fe coupling in the hydrides, while high-field experiments will show possible metamagnetic transitions, which provide further insight into the magnetic structure.

This paper is organized as follows. In Sec. II, we will give experimental details of our sample preparation and measurement techniques. Section III contains the successive experimental results of the magnetization measurements on four series of compounds, all ordering in the $La_6Co_{11}Ga_3$ structure type: $Nd_6Fe_{13}M$, $Nd_{6-x}La_xFe_{11}Al_3$, heavy-R substituted and hydrogenated compounds. In Sec. IV a model is constructed, describing the field dependence of the observed magnetization behavior. A spin structure is proposed in Sec. V, which explains most features of the $La_6Co_{11}Ga_3$ structure type in a straightforward manner. Finally, the main conclusions are presented in Sec. VI.

II. EXPERIMENTAL

The compounds, each with a weight of 15 g, were prepared by arc melting starting materials of at least 99.9% purity. After melting, the ingots were wrapped in Ta foil, sealed in an evacuated quartz tube and annealed for several weeks at temperatures ranging from 600 to 800 °C. The $Nd_6Fe_{13-x}M_{1+x}$ phase was shown by Grieb and Henig[12] for M=Al and Müller *et al.*[13] for M=Cu to form peritectically from the melt. The compound with M=Cu is a line phase with x=0 and a formation temperature as low as 600 °C. This makes it extremely hard to prepare $R_6Fe_{13}M$ com-

TABLE I. Preparation methods (annealing time/annealing temperature in °C/quenched) and crystallographic data and Néel temperature of the $R_6Fe_{13-x}M_{1+x}$ alloys ordering in the $La_6Co_{11}Ga_3$ structure. The uncertainty in the lattice parameters is of the order of 1 pm and in T_N 2 K.

Compound	Preparation	a [nm]	c [nm]	V[nm^3]	T_N [K]
$Nd_{6.1}Fe_{13}Au$	$2w/600/q$	0.8084	2.260	1.477	411
$Nd_{6.4}Fe_{13}Cu_{1.3}$	$2w/550/q$	0.8111	2.230	1.467	419
$Nd_{6.4}Fe_{13}Ag_{1.3}$	$3w/600/q$	0.8117	2.276	1.499	415
$Nd_{6.4}Fe_{13}Si_{1.3}$	$3w/600/q$	0.8054	2.281	1.480	421
$Nd_{6.1}Fe_{13}Ga_1$	$2w/700$	0.8072	2.295	1.495	433
$Nd_{6.1}Fe_{12}Ga_2$	$2w/700$	0.8092	2.298	1.504	373
$Nd_{6.1}Fe_{12.7}Ga_{1.3}$	$3w/675$	0.8077	2.298	1.499	417
$Nd_{6.0}Dy_{0.1}Fe_{12.7}Ga_{1.3}$	$3w/675$	0.8072	2.296	1.496	418
$Nd_{5.9}Dy_{0.2}Fe_{12.7}Ga_{1.3}$	$3w/675$	0.8071	2.295	1.495	418
$Nd_{5.6}Dy_{0.5}Fe_{12.7}Ga_{1.3}$	$3w/675$	0.8071	2.295	1.492	418
$Nd_{5.1}Dy_{1.0}Fe_{12.7}Ga_{1.3}$	$3w/675$	0.8056	2.286	1.484	420
$La_3Gd_3Fe_{11}Al_3$	$4w/600$	0.8156	2.336	1.553	a
$Nd_6Fe_{11}Al_3$	$4w/600$	0.8152	2.310	1.535	305
$Nd_3La_3Fe_{11}Al_3$	$4w/600$	0.8183	2.349	1.573	273
$La_6Fe_{11}Al_3$	$2w/800/q$	0.8220	2.382	1.609	230

[a]No ordering temperature observable.

pounds single phase and we will show that almost all compounds reported on in literature are contaminated to a certain (sometimes large) extent. To prepare almost single-phase compounds, we have varied the composition of the starting alloy and the annealing temperature. The best composition and heat treatment are reported in Table I together with the crystallographic data and magnetic ordering temperature. The lattice parameters were determined by x-ray diffraction using a Philips PW1800 with Cu-$K\alpha$ radiation. In the next sections will be referred to the stoichiometric compounds although the actual starting composition might be different. Hydrogenation was performed at room temperature at a hydrogen pressure of 1.3 bar. The hydrogen uptake was calculated from the weight difference with the unhydrogenated compound for $Nd_6Fe_{12}Ga_2$. A lattice expansion of 2.9 $\times 10^{-3}$ nm^3/H atom is observed. This value agrees with usual observations in intermetallics[14] and with findings of Leithe-Jasper et al.[15] in $R_6Fe_{13-x}M_{1+x}$ compounds. For the other compounds, the hydrogen uptake was calculated from the expansion of the lattice parameters compared to those of their parent compounds using 2.9×10^{-3} nm^3/H atom. For $R_6Fe_{13}M$ compounds with M=Au and Ag, the lattice expansion is approximately 3.3×10^{-3} nm^3/H atom (Ref. 15) and this latter value was used for the determination of the amount of hydrogen absorbed in these two compounds. The compounds are automatically decrepitated due to hydrogen absorption. After magnetic measurements, the lattice parameters were reexamined to exclude the possibility of hydrogen desorption during the measurement.

The field dependence of the magnetization was measured in the high-field installation at the University of Amsterdam.[16] The measurements were performed on free powders which were sieved in a 40 μm sieve to assure that the particles are single crystalline. The magnetization was measured both in quasi-stationary fields (constant during 0.1 s) as well as in fields increasing and decreasing linearly with time. Other magnetic measurements were made in a SQUID magnetometer in the temperature range 5–300 K in magnetic

fields up to 5.5 T, whereas above 300 K the magnetization was measured in a home-built magnetometer based on the Faraday principle, using polycrystalline lumps of material to prevent oxidation.

III. RESULTS AND DISCUSSION

A. $Nd_6Fe_{13}M$ compounds

In Fig. 1 we show the magnetization behavior above room temperature for $Nd_6Fe_{13}M$ compounds with M=Au, Ag, Cu, and Si. Although the atomic concentration of Cu and Ag is above 5% in the starting alloy (see Table I), no substitution on Fe sites is observed[13] and the compounds formed are very likely line compounds of composition $Nd_6Fe_{13}M$. All compounds show a cusplike anomaly around 415 K. Below 340 K, there is a moderate (M=Cu), small (M=Au) or no (M=Ag) increase in magnetization, reminiscent of the re-
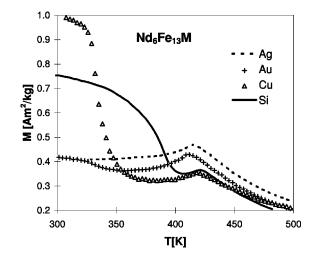

FIG. 1. Magnetization versus temperature for $Nd_6Fe_{13}M$ compounds, measured on polycrystalline bulk material in a field of 0.1 T.
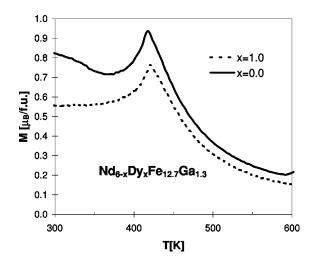
FIG. 2. Temperature dependence of the magnetization at 0.1 T of polycrystalline bulk material of $Nd_{6-x}Dy_xFe_{12.7}Ga_{1.3}$ compounds with $x=0$ and 1.

FIG. 3. Field dependence of the magnetic moment at 4.2 K of $Nd_6Fe_{13}M$ compounds with $M=$Ag, Cu, and Si, measured on free-powder material. The lines correspond with data taking during continuous sweeps with increasing and decreasing field. The symbols correspond to data taken in quasistationary fields in decreasing field.

sults reported by Weitzer et al.[5] However, for $M=$Au the increase at 340 K is a factor of 10 smaller than in a sample of the same composition, prepared by us earlier[7] and more than 100 times smaller than in Ref. 5. Mössbauer-effect measurements made on the sample with $M=$Au have already shown that magnetic ordering exists up to 420 K.[7] This excludes the ferromagnetic ordering proposed in Ref. 5. The fact that the magnetization near 340 K can be changed by a factor of 100, is a clear indication that this increase is not intrinsic to the compound, but that it is due to a ferromagnetic impurity. Nd_2Fe_{17}, being the neighboring compound in the phase diagram and having a Curie temperature of 326 K,[17] is the obvious candidate. In fact, it can be shown that the presence of less than 1% of this phase is sufficient to cause the rise in magnetization in $Nd_6Fe_{13}Cu$. Such small amounts can easily escape detection by x-ray diffraction and Mössbauer spectroscopy. These considerations prove that these compounds are antiferromagnets (or almost compensated ferrimagnets) with an ordering temperature around 415 K.

The temperature dependence of the magnetization we measured for $Nd_6Fe_{13}Si$ is quite similar to the curve measured by Yan et al.[6] These authors consider their compound to be a ferrimagnet and the dip in the magnetization versus temperature curve is perceived as a compensation point. Again, with this sample the increase of magnetization is strongly dependent on the preparation. In the light of these and the previous remarks, it is therefore much more likely that this compound is also an antiferromagnet with a small amount of magnetic impurity. Assuming Nd_2Fe_{17} to be the impurity, the increase in the Curie temperature is understandable as R_2Fe_{17} compounds are well known to show an enhancement of Curie temperature upon Si substitution.[18] The increase of magnetization and T_C, being 399 K, would correspond with the presence of approximately 0.5 wt. % of $Nd_2Fe_{16}Si$ in $Nd_6Fe_{13}Si$.[19] Such a small amount may even escape detection by neutron diffraction.[6] It is probably this solubility of Si in R_2Fe_{17} that makes it so difficult to prepare $Nd_6Fe_{13}Si$ single phase. Because Ga can substitute Fe on the $16l_2$ site, some excess Ga can be added that prevents the presence of impurities. The compounds $Nd_{6-x}Dy_xFe_{12.7}Ga_{1.3}$
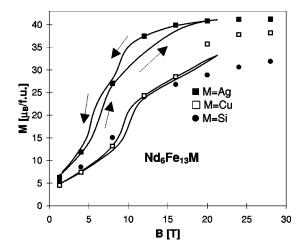
are therefore single phase with a clear antiferromagnetic ordering temperature as is shown in Fig. 2.

High-field measurements on $Nd_6Fe_{13}M$ compounds with $M=$Au, Ag, Cu, and Si are done on a different series of compounds of stoichiometric starting composition. Therefore, they all show small amounts of Nd_2Fe_{17} impurity ($\leqslant 1$ wt. %), but in the magnetization versus field behavior their influence is limited. The results obtained on compounds with $M=$Ag, Cu, and Si are shown in Fig. 3. The measurements resemble those of $Nd_6Fe_{12}Ga_2$ (Ref. 10) and $Nd_6Fe_{13}Au$ (Ref. 7): a two-step magnetization behavior indicating a change from almost antiferromagnetic to full ferromagnetic alignment. The origin of the hysteresis will be explained in Sec. IV. The saturation magnetization and critical fields belonging to these steps are collected in Table II. In the behavior of $Nd_6Fe_{13}Si$, we see the ''low'' field transition at 7.8 T. This agrees with the value found for the metamagnetic-transition field by Allemand et al.[2] and B_0^{cr2} of Yan et al.[6] A transition at even lower fields as reported by the latter authors is not visible.

The sample with $M=$Au is easily saturated and the total magnetic moment at 28 T is $42.5\mu_B$/f.u. Assuming the Nd moment to have its free-ion value, an average Fe moment of $1.8\mu_B$ is derived. This is somewhat lower then data from Mössbauer spectroscopy[20,5] giving an average Fe moment of

TABLE II. Magnetization at 28 T and critical fields B_1 and B_2 of $Nd_6Fe_{13}M$ compounds. B is determined by taking the maximum in the susceptibility in decreasing field. The free-ion value for the Nd moment has been used in the calculation of the Fe moment.

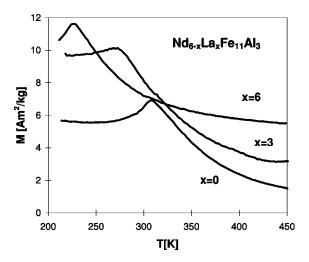| M	M [μ_B/f.u.]	μ [μ_B/Fe]	B_1 [T]	B_2 [T]
Au	42.5(2)	1.8(1)	4.7(1)	8.0(2)
Ag	41.2(2)	1.7(1)	5.1(1)	8.7(2)
Cu	38.2 (2)	1.4(1)	9.2(1)	18(1)
Si	>32	$\geqslant 1$	7.8(1)	>20
Ga	41.9(2)	1.7(1)	7.7(1)	16.8(2)

FIG. 4. Temperature dependence of the magnetization of the compounds $Nd_{6-x}La_xFe_{11}Al_3$ with $x=0$, 3, and 6 showing the Néel temperature. Measurements were performed on polycrystalline bulk material in a field of 1 T.
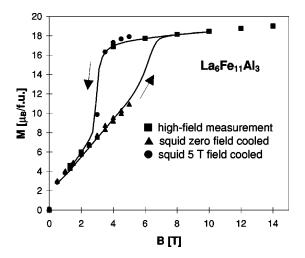

FIG. 5. Field dependence of the magnetic moment at 4.2 K of free powder of $La_6Fe_{11}Al_3$. The line corresponds with data taking during continuous sweeps with increasing and decreasing field. For the meaning of the symbols see figure.

$2.0\mu_B$ at low temperatures [derived from the hyperfine splitting using a conversion factor of 1.48 T/μ_B (Ref. 21)]. For the other compounds, the magnetization is considerably lower, while Mössbauer spectroscopy indicates an Fe moment independent of the M atom. It is possible that the M atom is responsible for a deviation of the magnetic moment of the Nd-ion from the free-ion value. Neutron-diffraction experiments[6] give indeed very low values of $0.5\mu_B$/Nd for $Nd_6Fe_{13}Si$ at room temperature. It is, however, also possible that even for $M=Au$ and Ag higher fields are needed for complete saturation magnetization.

For $M=Au$ and Ag, the magnetization is saturated in fields below 20 T, which means that the antiferromagnetic coupling between the sublattices is very weak. For $M=Si$ and Cu, the low-field susceptibility is considerably lower, indicating a stronger, although still weak, coupling between the sublattices. Besides its influence on the reduced magnetization of the R moments, the M atom has therefore also an impact on the strength of the antiferromagnetic coupling. The origin of this impact will be discussed shortly in Sec. V.

B. $Nd_{6-x}La_xFe_{11}Al_3$ compounds

While the Néel temperature is not influenced by the kind of stabilizing atom, it is strongly influenced by its concentration, as can be seen from the compounds with increasing Ga-concentration (Table I). Both dilution and reduction of the Fe moment due to mixing of $3d$ states with valence-electron states of Ga are responsible. In Ref. 10, it is reported that substitution of La for Nd in $Nd_6Fe_{12}Ga_2$ leads to a small decrease of the Néel temperature.

In $R_6Fe_{11}Al_3$ compounds ($R_6Fe_{11}Ga_3$ compounds do not exist), the intra Fe-sublattice interaction is further decreased and the importance of the R elements in determining the ordering temperature is even more evident. This can clearly be seen in Fig. 4, where the temperature dependence of the magnetization is displayed for $Nd_{6-x}La_xFe_{11}Al_3$ compounds with $x=0$, 3, and 6. The Néel temperature is discernible as the maximum in the magnetization. The value of 305 K derived for $x=0$ is in good agreement with the value found

from Mössbauer-effect spectroscopy [308 K (Ref. 22)]. For decreasing Nd concentration the Néel temperature decreases rapidly and $T_N=230$ K for $x=6$. Local fluctuations in La/Nd ratio may be responsible for the shallowness of the maximum for $x=3$. For $Nd_3La_3Fe_{11}Al_3$, a further decrease in magnetization is seen around 350 K in lower fields, which we ascribe to $Nd_2Fe_{17-x}Al_x$ impurity. For $La_6Fe_{11}Al_3$, some magnetization remains present above T_N, which corresponds to about 2 wt. % of α-Fe (La_2Fe_{17} does not exist).

The field dependence of the magnetization of $La_6Fe_{11}Al_3$ has been measured by Hu et al.[9] who found no hysteresis. These authors conclude that the absence of any R-sublattice anisotropy is responsible for this. The hysteresis in the other compounds is explained by pinning of narrow domain walls which is due to the strong crystal-field-induced anisotropy of the R sublattice. Calculations of Li et al.[23] show indeed large second-order crystal-field coefficients for both R sites. We also measured this compound in high fields, and Fig. 5 shows that the results are completely different from the results of Hu et al.

With increasing field, a metamagnetic transition near 6 T to full parallel alignment is found. When the field is decreased a very large hysteresis is present. To confirm that the hysteresis is intrinsic to the compound and not due to the large sweep rate in the high-field experiments, we also measured the magnetization in a SQUID magnetometer. When the maximum field is below the metamagnetic transition, as is the case in our SQUID measurements and the vibrating sample magnetometer (VSM) measurements of Hu et al.,[9] there will be no hysteresis in decreasing field. However, when the sample is cooled from room temperature to 5 K in a magnetic field of 5 T, the magnetic data agree perfectly with the high-field measurement in decreasing field. This is because the transition field for ferromagnetic alignment is zero at the ordering temperature (230 K) and the sample cooled in a magnetic field of 5 T is therefore already saturated. From these measurements it can be concluded that the Fe moments are ordered in at least two antiferromagnetically coupled sublattices and that the hysteresis is also due to the Fe-sublattice anisotropy. In Sec. IV, we will show that the
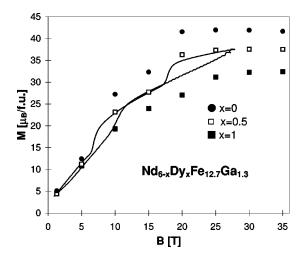
FIG. 6. Field dependence of the magnetic moment at 4.2 K of free powder of $Nd_{6-x}Dy_xFe_{12.7}Ga_{1.3}$ compounds with $x=0$, 0.5, and 1.0. The line corresponds with data taking during continuous sweeps with increasing and decreasing field. Symbols correspond to data taken in quasistationary fields in decreasing field.

FIG. 7. Field dependence of the magnetic moment at 4.2 K of free powder of $La_3Gd_3Fe_{11}Al_3$. Symbols correspond to data taken in quasistationary fields in decreasing field. The line is a linear fit to the data, based on Eq. (7).

experimentally observed magnetization behavior can be well understood in terms of a theoretical model based on local minimization of the free energy. The hysteresis can be explained by taking into account the second-order magnetocrystalline anisotropy of the Fe sublattice only.

A rather similar field dependence of the magnetization is found in $LaFe_{13-x}Al_x$ compounds with $1 \leqslant x \leqslant 1.8$ by Palstra et al.[24] (note the much smaller amount of La). This cubic compound is also an antiferromagnet with ordering temperature around 190 K (an unidentified anomaly at 230 K may well correspond to the $La_6Fe_{13-x}Al_{1+x}$ phase). At 4.2 K, a field of 4 T is required in increasing field to induce a metamagnetic transition from antiparallel alignment to parallel alignment, while in decreasing field the transition appears at only 0.6 T. These authors show that the transition is accompanied by a large forced volume magnetostriction of almost 1%. This might cause the observed hysteresis, but it is possible that the hysteresis in these compounds is also due to the magnetocrystalline anisotropy of the Fe sublattice.

C. Substitution of heavy-R elements

To study the influence of the R sites on the magnetization, we substituted some heavy-R elements, Dy and Gd, for Nd. Figure 6 shows the magnetization behavior of the $Nd_{6-x}Dy_xFe_{12.7}Ga_{1.3}$ compounds with $x=0$, 0.5, and 1.0 and Fig. 7 shows the behavior of $La_3Gd_3Fe_{11}Al_3$. At 35 T, the magnetization of the Dy-substituted compounds is still lower than of the parent compound (Table III). As the free-ion moment of Dy is much higher than of Nd ($10\mu_B$ and $3.28\mu_B$, respectively), it is clear that full parallel alignment of the moments is not reached in the Dy-substituted compounds. This means that the R-Fe coupling, which is ferromagnetic for light-R and antiferromagnetic for heavy-R elements, as explained by Campbell,[25] is strong in the $R_6Fe_{13}M$ compounds as it is in other R-T compounds. This contradicts assumptions of weak coupling to the Fe sublattice[11,9] or even ''non-Campbell'' type coupling.[26]

The difference in magnetization at 35 T between $Nd_{6-x}Dy_xFe_{12.7}Ga_{1.3}$ with $x=0$ and 1 is $9.2\mu_B$, significantly
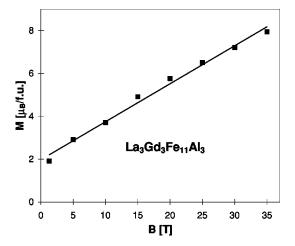
smaller than $13.3\mu_B$, which is expected when all Dy moments are antiparallel aligned to the Fe and Nd moments and the applied field. Because the susceptibility at 35 T is approximately zero for both compounds, it is not likely that a rotation of the Dy moments is already occurring. Taking into account the crystal structure,[27] an explanation is proposed: the $8f$ R site has 12 Fe nearest neighbors and a strong coupling to the Fe moment might not be surprising. The $16l$ R site, on the other hand, has only 4 Fe and 8 other $16l$ sites as nearest neighbors. It seems therefore possible that only the moments at the $8f$ site are strongly coupled to the Fe moments, while the ions at the $16l$ site behave (almost) paramagnetically. To agree with the experimental results, this proposal requires a strong preferential occupancy of the $8f$ site by Dy, which is possible because the $8f$ site is much smaller than the $16l$ site.

A most important feature of the Dy- and Gd-substituted compounds is the unchanged magnetization of about $2\mu_B$ at zero field. Whether the $16l$ site moments are paramagnetic, antiparallel, or parallel to the $8f$ site moments, the zero-field magnetization would have been altered significantly compared to the compounds with $R=$Nd. (Only when exactly 2/3 of the Dy and Gd atoms substitute at the $8f$ site, antiparallel alignment would not change the zero-field magnetization. This is very unlikely to be true for the whole substitution range $x=0.5$, 1.0, and 3.0.) We therefore propose a different magnetic structure: the moments at the $8f$ site are arranged

TABLE III. Magnetization at 35 T and critical fields measured in decreasing field of $Nd_{6-x}Dy_xFe_{12.7}Ga_{1.3}$ and $La_{6-y}Gd_yFe_{11}Al_3$ compounds. The free-ion values for the R moments have been used in the calculation of the Fe moment.

Compound	M [μ_B/f.u.]	μ [μ_B/Fe]	B_1 [T]	B_2 [T]
$x=0.0$	41.6(2)	1.7(1)	5.8(1)	14.1(2)
$x=0.5$	37.5(2)	1.9(1)	6.7(1)	17.8(2)
$x=1.0$	32.4(2)	2.1(1)	9.2(1)	>20
$y=0.0$	18.9(1)	1.7 (1)	2.9(1)	
$y=3.0$	>8	$\geqslant$1		

TABLE IV. Crystallographic and magnetic data of the $Nd_6Fe_{13-x}M_{1+x}$ hydrides ($La_6Co_{11}Ga_3$ structure; space-group $I4/mcm$). M is magnetization at 5 T. The uncertainty in the values of the lattice parameters is of the order of 1 pm.

Compound	a [nm]	c [nm]	V [nm^3]	dV [nm^3]	y	EMD	M_s [μ_B/f.u.]	T_C [K]
$Nd_6Fe_{13}AuH_y$	0.8084	2.527	1.651	0.174	15		41.5(1)	
$Nd_6Fe_{13}AgH_y$	0.8198	2.535	1.706	0.207	18	EA	36.8(1)	(487)
$Nd_6Fe_{12.7}Ga_{1.3}H_y$	0.8136	2.521	1.668	0.169	15	EA	40.1(1)	458
$Nd_{5.8}Dy_{0.2}Fe_{12.7}Ga_{1.3}H_y$	0.8127	2.522	1.665	0.170	15	EA	38.0(1)	460
$Nd_{5.5}Dy_{0.5}Fe_{12.7}Ga_{1.3}H_y$	0.8112	2.518	1.657	0.165	14	EA	34.8(1)	455
$Nd_{5.0}Dy_{1.0}Fe_{12.7}Ga_{1.3}H_y$	0.8086	2.517	1.642	0.158	14	EA	30.5(1)	441
$Nd_6Fe_{11}Al_3H_y$	0.8165	2.521	1.681	0.146	13	EA	33.6(1)	(428)
$Nd_3La_3Fe_{11}Al_3H_y$	0.8264	2.581	1.763	0.190	16	EA	27.8(1)	442
$La_6Fe_{11}Al_3H_y$	0.8291	2.604	1.789	0.180	16	EA	22.7(1)	(444)

such that half of the moments point up and the other half down. In Sec. V, it is explained how such a spin structure may arise. Whether the spontaneous magnetization of about $2\mu_B$/f.u. is intrinsic to the $R_6Fe_{13}M$ compounds remains questionable.

D. Hydrides

It was shown in 1994 by Coey *et al.*[4] that $R_6Fe_{13}M$ compounds absorb hydrogen without any change in the crystal symmetry and structure type. This work was extended by Leithe-Jasper *et al.*[15] In the present work we have hydrogenated compounds in which the light-R elements Nd and Pr are replaced by the nonmagnetic La or the heavy-R Dy. Because no low-temperature magnetization data are available for $R_6Fe_{13}M$ hydrides with $M=$ Au and Ag, we also prepared these hydrides. Crystallographic and magnetic data of all compounds are collected in Table IV. All compounds are hydrogenated without any external heating. However, the absorption reaction is exothermic and the released heat increases the temperature of the sample, further stimulating the reaction. During the reaction, the temperature increased to approximately 100 °C. The amount of hydrogen in the compound is determined by assuming that the lattice expansion
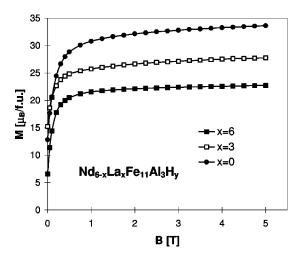
totals 2.9×10^{-3} nm^3/H atom as is explained in Sec. II. For $Nd_6Fe_{12.8}Ga_{1.2}$, Yartys *et al.*[28] find 20 hydrogen atoms/f.u. This significantly higher value indicates that the hydrogenation reaction at room temperature may be incomplete.

The magnetization behavior displayed in Fig. 8 shows that all hydrides with light or nonmagnetic R elements show ferromagnetic behavior as previously reported.[4,15,28] For $La_6Fe_{11}Al_3H_{16}$, the Fe moment can be unambiguously calculated to be $2.1\mu_B$, much higher than the $1.7\mu_B$ in the parent compound. Assuming the same Fe moment of $2.1\mu_B$ in $Nd_6Fe_{11}Al_3H_{13}$, a Nd moment of $1.8\mu_B$ is derived from the experimental data. In $Nd_6Fe_{13}AuH_{15}$, an average Fe moment of $2.35\mu_B$ is found in Mössbauer-effect measurements.[15] Taking this value for the Fe moment, again, a Nd moment of $1.8\mu_B$ is required to fit the magnetic data. We may therefore conclude that the hydrogen absorption reduces the Nd moment by a fairly large amount. The even lower magnetization in $Nd_6Fe_{13}AgH_{18}$ is probably due to a further reduction of the Nd moment as this compound has absorbed more hydrogen than the compound with $M=$ Au. It has been suggested that the absorbed hydrogen is firmly bound in the R sheets of the structure.[15]

The magnetization behavior of the hydrides in which Nd is partly replaced by Dy (see Fig. 9) shows a decreasing

FIG. 8. Field dependence of the magnetization at 5 K for free powders of $Nd_{6-x}La_xFe_{11}Al_3H_y$ compounds. The lines are guides to the eye.
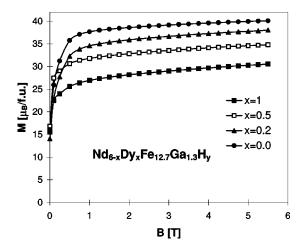

FIG. 9. Field dependence of the magnetization at 5 K for free powders of $Nd_{6-x}Dy_xFe_{12.7}Ga_{1.3}H_y$ compounds. The lines are guides to the eye.
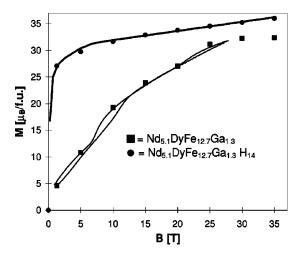
FIG. 10. Field dependence of the magnetization at 4.2 K of free powder of $Nd_5Dy_{1.0}Fe_{12.7}Ga_{1.3}$ and $Nd_5Dy_{1.0}Fe_{12.7}Ga_{1.3}H_{14}$. Line through the data points on the latter sample is a guide to the eye.

saturation magnetization with increasing amount of Dy. This indicates that, as in the parent compounds, the heavy-R moments are antiferromagnetically coupled to the Fe moments. The high-field measurements made on $Nd_{5.0}Dy_{1.0}Fe_{12.7}Ga_{1.3}H_{15}$, plotted in Fig. 10, do not show any transition, but a steady increase in magnetization, which may be due either to the rotation of the Dy moment or to an increase of the reduced Nd moment.

The compounds were all magnetically aligned and the easy magnetic direction (EMD) was determined by x-ray diffraction. All compounds show a clear easy-axis anisotropy, an example of which is given in Fig. 11. Because also $La_6Fe_{11}Al_3H_{16}$ has easy-axis magnetization, it is clear that the room-temperature anisotropy is due to the Fe sublattice. An increase in magnetization at lower temperatures as shown in Fig. 12, may indicate a spin-reorientation transition from easy-axis anisotropy at room temperature to easy-plane anisotropy at cryogenic temperatures, but could not be confirmed by x-ray diffraction.

IV. CALCULATED MAGNETIZATION

All compounds show considerable or even very large hysteresis in the magnetization versus field behavior. In most
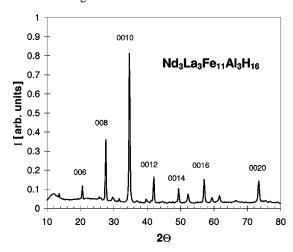

FIG. 11. Room-temperature Cu-$K\alpha$ x-ray-diffraction pattern of a magnetically aligned $Nd_3La_3Fe_{11}Al_3H_{16}$ sample.
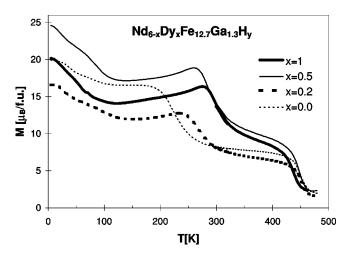

FIG. 12. Temperature dependence of the magnetization at 0.1 T of $Nd_{6-x}Dy_xFe_{12.7}Ga_{1.3}H_y$ compounds with $x = 0$, 0.5, and 1.0 showing Curie temperature and possible spin-reorientation temperature. Data below 300 K are on free powder, above 300 K on polycrystalline bulk material.

ferrimagnetic heavy-R-Fe compounds, the antiferromagnetic R-Fe coupling is rather strong and hysteresis due to the magnetocrystalline anisotropy is just a small effect. However, the antiferromagnetic coupling in the $R_6Fe_{13-x}M_{1+x}$ compounds (R is nonmagnetic or light rare earth) is extremely weak. In these compounds, the magnetocrystalline anisotropy plays therefore an important role in the determination of the magnetization behavior, leading to large hysteresis. We will show that a model based on local energy minimization is able to reproduce the measured curves in an excellent way.

Zhao et al.[29] have calculated the field dependence of the magnetization for single crystals that are free to rotate in the applied field, using a global energy minimization in a two-sublattice model. In the case that both sublattices have easy-plane anisotropy, the rotation of the magnetization takes place within the basal plane and the magnetic anisotropy will not appear in the energy expression. In the case that one of the sublattices has easy-axis anisotropy and the other an arbitrary type of anisotropy, the rotation of the magnetization vectors is in a single plane intersecting the c axis.[30] Then, the following expression for the total energy of the system is valid:

$$E = K_1^R \sin^2\theta + K_2^R \sin^4\theta + K_3^R \sin^6\theta + K_1^T \sin^2(\theta + \alpha)$$

$$+ K_2^T \sin^4(\theta + \alpha) + n_{RT} M_R M_T \cos\alpha - BM, \quad (1)$$

$$M = \sqrt{M_R^2 + M_T^2 + 2 M_R M_T \cos\alpha} \quad (2)$$

with θ the angle between M_R and the c axis and α the angle between M_R and M_T. The two sublattices are labeled R and T, but we wish to stress that these need not necessarily represent the rare-earth and transition-metal sublattice. Zhao et al.[29] have used Eq. (1) to calculate the global energy minimum and the associated angles and magnetization M as a function of applied field B. It is clear that in calculations based on global energy minimization, no hysteresis will appear. However, the magnetic anisotropy may cause energy barriers, which prevent the rotation of the magnetization to the global minimum. We therefore have extended the model
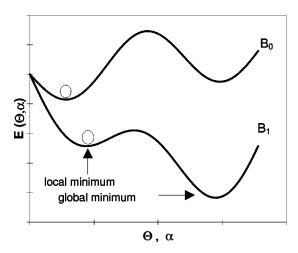
FIG. 13. Schematic representation of the free energy versus angle of magnetization for two different applied fields, showing the difference between global and local minimization.

FIG. 14. Calculated (dashed) and experimental (full) magnetization behavior at 4.2 K on free powder of $\text{La}_6\text{Fe}_{11}\text{Al}_3$ in increasing and decreasing field. The parameters used for the calculation are given in the figure.

by calculating the local minimum as a function of the applied field. This is schematically represented in Fig. 13.

Starting from the global minimum in zero field, we have increased the field and calculated the energy around the zero field minimum by varying the two independent parameters, θ and α. When the energy in a neighboring point is lower, this point is taken as the new starting point and the procedure is repeated. When all neighboring points have higher energy, the point is considered to be the local minimum. The neighboring points are chosen to be 0.2° apart. Because of the smoothness of all energy terms involved, there is no risk of missing the descend to the local minimum. This method leads very easily and efficiently to the local minimum. The steps have the effect of a small activation energy which causes the rotation of the magnetization to happen fractionally earlier than results from a steepest-descend method would give. Because the local minimum is calculated, the magnetization in increasing field may differ from the magnetization in decreasing field. Whenever a first-order magnetization process appears with increasing field, the calculation will show hysteresis between the increasing- and decreasing-field curve. The size of the hysteresis depends on the anisotropy terms.

In the next section, we will propose a spin structure for the $R_6\text{Fe}_{13-x}M_{1+x}$ compounds, consisting of Fe sheets antiferromagnetically coupled to each other. The T in Eqs. (1)–(3) should therefore be read as Fe, and R as Fe$'$ and both sublattices will have the same magnetization and anisotropy. Figure 14 shows the magnetization behavior of $\text{La}_6\text{Fe}_{11}\text{Al}_3$ shown earlier in Fig. 5, but now together with the calculated magnetization. Besides an offset of $1.5\mu_B$/f.u. which is likely due to α-Fe impurity, only three free parameters have been used to produce the calculated curve. The magnetization of the sublattices, the antiferromagnetic exchange coupling, and the second-order anisotropy constant K_1. The sublattice magnetization of $8.5\mu_B$ corresponds to $1.58\mu_B$/Fe (corrected for the amount of impurity) in good agreement with the value of $1.60\mu_B$/Fe inferred from Mössbauer-effect spectroscopy.[9] The value of the anisotropy constant corresponds to 0.2 MJ/m^3, which is a physically realistic value for Fe-sublattice anisotropy in intermetallics, comparable with, e.g.,
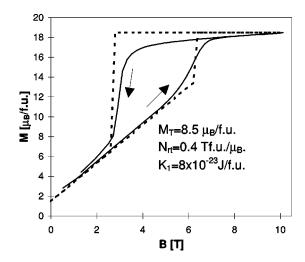
0.7 MJ/m^3 in $\text{La}_2\text{Fe}_{14}\text{B}$. The derived value for the antiferromagnetic $n_{\text{FeFe}'}$ coupling is very small as expected from considerations made in the former section.

When, as in the SQUID and VSM measurements, the maximum field is lower than the transition field, measured with increasing field, no hysteresis will occur. By introducing more anisotropy terms and by allowing the sublattices to have independent parameters, the fit to the measured curve will of course increase, but the improvement will be marginal. It should be noted that introducing ferrimagnetic sublattices leads to a spontaneous magnetization. However, it also leads to zero susceptibility at low fields, not in agreement with the measured curves. For the compounds with magnetic R elements instead of La, the magnetization curves are far more complicated as can be seen in Figs. 3 and 6. We can nevertheless reproduce the magnetization behavior in most $R_6\text{Fe}_{13-x}M_{1+x}$ compounds rather well by allowing one sublattice to have easy-axis (EA) anisotropy ($K_1>0$) and the other easy-plane ($K_1>0 \wedge K_1+K_2<0$). The parameters in the calculations of Fig. 15 are chosen such that the magnetization curve resembles $\text{Nd}_6\text{Fe}_{13}\text{Au}$. The two-step magnetization behavior including the shape of the hysteresis can thus be explained by a two sublattice model. From Mössbauer spectroscopy it is, however, concluded that the Fe-sublattice moment in $\text{Nd}_6\text{Fe}_{13}M$ compounds with $M=\text{Au}$, Ag, and Cu lies in the basal plane both at room temperature and 5 K.[5] In the case that all sublattices have basal plane anisotropy ($K_1<0 \wedge K_1+2K_2<0$) no hysteresis is expected at all, except when the anisotropy depends on the magnetization direction within the plane. In that case, the energy of the system is given by

$$E=K_2^R{}' \cos 4\theta+K_2^T{}' \cos 4(\theta+\alpha)+n_{RT}M_RM_T \cos \alpha-BM \tag{3}$$

with θ now being the angle between the a axis and M_R and α still the angle between M_R and M_T. Assuming this to be the case, the measured magnetization curves can be reproduced even in the case that both sublattices are identical. A calculated magnetization curve of this kind is also plotted in
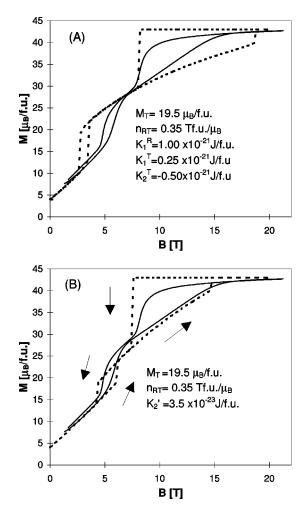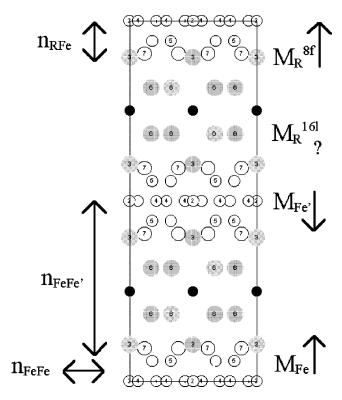
FIG. 16. view of the $R_6Fe_{13-x}M_{1+x}$ structure along the a axis, showing the proposed magnetic structure and exchange interactions involved. The full spheres are M atoms, the grey spheres R atoms at $8f$ site (3) and $16l$ site (6), and the open spheres are the Fe atoms.

FIG. 15. Calculated (dashed) and experimental (full) magnetization behavior at 4.2 K on free powder of $Nd_6Fe_{13}Au$ in increasing and decreasing field. Curve (A) is calculated using an easy-axis and an easy-plane sublattice. Curve (B) has two identical sublattices with planar anisotropy. The parameter values and units are displayed in the figure. An offset of $4\mu_B$ has been included in both calculated curves.

Fig. 15. In both calculated cases, a high-field jump in increasing field is necessary to create hysteresis. However, this jump is not visible in most of the measured curves. This is most likely due to the smearing out of the transition fields, as was also observed for $La_6Fe_{11}Al_3$. Nucleation of reversed domains at points with higher local demagnetization or smaller local anisotropy will, as in permanent magnets, reduce and smear out the sharp transitions in these compounds. The calculations show that very complicated magnetization behavior can be understood in a simple model of minimizing the local energy in a two-sublattice model. With a few precautions, this model can be extended to incorporate a third independent angle. In that case, no restrictions on the easy-axis of magnetization (EMD) of the sublattices are required.

V. SPIN STRUCTURE

From Sec. III, a number of conclusions about the exchange interaction may be drawn. As $La_6Fe_{11}Al_3$ has also almost no net magnetization, it is clear that the Fe sublattices are coupled antiparallel. Fitting the measured curves with a

two-sublattice model yields an extremely weak antiferromagnetic coupling strength of approximately 0.4 Tf.u./μ_B. From the heavy-R-substituted compounds, it follows that the R-Fe coupling is rather strong; both in the parent compound and the hydride, the Dy and Fe moments are still antiparallel at 35 T. We also suggested that the R atoms at the $8f$ site (strongly coupled to the Fe moments) have half the moments up and the other half down, while the $16l$ site moments are paramagnetic. [A weak antiferromagnetic R-R interactions between the $16l$ site moments would explain the second antiferromagnetic ordering found in $Nd_6Fe_{12}Ga_2$ at 23 K (Ref. 10).]

The results discussed so far, very much favor the spin structure as proposed by Kajitani et al.:[8] The Fe moments in the sheets around $c=0$ and 1/2 are strongly ferromagnetically coupled, whereas the coupling between the Fe sheets is antiferromagnetic across the M layer at $c=1/4$. In this structure, the R moments at the $8f$ site will couple in the usual (ferromagnetically for light-R, ferrimagnetically for heavy-R) way to the moments of the Fe neighbors. The R moments at the $16l$ site may be weakly or not at all coupled to the other moments. This is schematically represented in Fig. 16. This proposed magnetic structure would be rather similar to the one found in YMn_2Ge_2 compounds.[31,32] Recently neutron-diffraction experiments on $ErFe_6Ge_6$ also suggest ferromagnetic Fe sheets, which couple antiferromagnetically across the layer.[33] Because of the large distance between the Fe sheets (≥ 8 Å) as compared to 4 Å in $ErFe_6Ge_6$ and 2.8 Å for the Mn sheets in YMn_2Ge_2, this structure seems unlikely at first view. It is nevertheless appealing as it explains many features.

First of all, this structure explains the very weak nature of the antiferromagnetic coupling, hereafter named interlayer coupling $n_{\text{FeFe}'}$. From the magnetization curve of La$_6$Fe$_{11}$Al$_3$ in Fig. 5 a value of $n_{\text{FeFe}'}=0.4$ T f.u./μ_B is derived. It also explains the low susceptibility in Gd$_3$La$_3$Fe$_{11}$Al$_3$ in Fig. 7. In the case of antiferromagnetically coupled Fe sublattices ($M_{\text{Fe}}=M_{\text{Fe}'}=M_{s,\text{Fe}}/2$) and neglecting anisotropy, Eq. (1) reduces to

$$E=n_{\text{FeFe}'}M_{\text{Fe}}^2\cos\alpha-BM, \qquad (4)$$

with $M=M_{\text{Fe}}\sqrt{2+2\cos\alpha}$. Minimizing this equation with respect to α gives

$$M/B=\frac{1}{n_{\text{FeFe}'}}. \qquad (5)$$

As the coupling between the R and the Fe moments $n_{R\text{Fe}}$ is so much larger than $n_{\text{FeFe}'}$, we may assume that the R-Fe coupling is rigidly parallel (light-R) or antiparallel (heavy-R) at any feasible field. The magnetization of the Gd-substituted compound may then be approximated by

$$M=|M_{\text{Fe}}-M_{\text{Gd}}|\sqrt{2+2\cos\alpha} \qquad (6)$$

with $M_{\text{Gd}}=M_{s,\text{Gd}}/2=10.5\mu_B$. Minimizing Eq. (4) with M given by Eq. (6), leads to

$$M/B=\frac{(M_{\text{Fe}}-M_{\text{Gd}})^2}{M_{\text{Fe}}^2}\times\frac{1}{n_{\text{FeFe}'}}. \qquad (7)$$

Thus, with an unchanged $n_{\text{FeFe}'}$ a much smaller susceptibility is expected and is also experimentally found. Using the Fe moment ($8.5\mu_B$) and $n_{\text{FeFe}'}$ of the fit to La$_6$Fe$_{11}$Al$_3$, the fit to the experimental curve of Gd$_3$La$_3$Fe$_{11}$Al$_3$ in Fig. 7 gives $M_{\text{Gd}}=6.2\pm0.5\mu_B$ or $10.8\pm0.5\mu_B$. Both solutions can have a physical explanation. When only the $8f$ site moments couple to the Fe moments, a preferentially and almost complete occupation of this site by Gd would lead to the former value. The latter value corresponds to the case that the Gd moments at both sites couple antiferromagnetically with the moments of the nearest Fe sheet. It should be noted that this does not lead to a compensation point in the temperature dependence of the magnetization, because each ferrimagnetic sublattice is coupled antiferromagnetically to its counterpart. Both schemes are therefore possible and the measurements are not able to distinguish between them. The low susceptibility of Gd$_3$La$_3$Fe$_{11}$Al$_3$ is, however, in both cases a necessary consequence of the proposed spin structure. The same mechanism also applies to the Dy-substituted compounds in Fig. 6. It explains the smaller susceptibility and higher transition fields in the magnetization versus field curves of the substituted compounds compared with the parent compound Nd$_6$Fe$_{12.7}$Ga$_{1.3}$.

In mean field theory, the ordering temperature of an intermetallic compound with two identical sublattices may be written in the following form:[34]

$$T_C=C_{\text{Fe}}(n_{\text{FeFe}}+|n_{\text{FeFe}'}|) \qquad (8)$$

with C_{Fe} the Curie constant of one sublattice. The sign convention is such that $n_{\text{FeFe}}>0$ means ferromagnetic intra-

sublattice interaction, and $n_{\text{FeFe}'}>0$ antiferromagnetic intersublattice interaction. For La$_6$Fe$_{11}$Al$_3$, the Néel temperature of 230 K corresponds with $n_{\text{FeFe}}+n_{\text{FeFe}'}=74$ T f.u./μ_B whereas $n_{\text{FeFe}'}$ is only 0.4 T f.u./μ_B. The ordering temperature is therefore completely determined by the strength of the intrasublattice interaction. The type of M atom does have a large influence on $n_{\text{FeFe}'}$ as can be seen in Fig. 3. Because the $4a$ M site is located between the Fe sheets, it may easily change the interlayer coupling, which is responsible for the antiferromagnetic interaction. The intralayer coupling n_{FeFe} is not expected to be influenced a great deal by the M atom. It is therefore clear that a change in the interlayer-coupling strength by the M atom will have almost no influence on the ordering temperature. This agrees with the experimental observations that the ordering temperature is almost independent of the type of M atom (see Table I).

By hydrogenation of the compound, an enormous expansion of the lattice occurs along the c axis, while the expansion in the a direction is very limited. This increase of the interlayer distance may lead to the disappearance of the antiferromagnetic interlayer coupling similar to the case of RMn$_2$Ge$_2$ compounds, where the interlayer coupling changes sign above a critical distance. With $n_{\text{FeFe}'}\leq0$, the hydrogenated compounds become ferromagnetic. The Curie temperature of the hydrides is, however, still given by Eq. (8). The Curie temperature of the hydrides should therefore be roughly equal to the Néel temperature of the parent compound. An increase of the Fe moments upon hydrogenation, as is derived both from magnetic measurements and from Mössbauer spectroscopy[4] will, however, lead to an increase of the ordering temperature. This effect is especially large for La$_6$Fe$_{11}$Al$_3$ as the ordering temperature in this compound is determined by the Fe-Fe interaction only. Assuming n_{FeFe} to remain constant, the increase in Fe moment from 1.6 to 2.1 μ_B will lead to a Curie temperature of the hydride of 380 K, reasonably close to the experimental value. For the other compounds, the R-Fe should be incorporated in Eq. (8), which will reduce the effect of an increased Fe moment. For the Nd$_{6-x}$Dy$_x$Fe$_{12.7}$Ga$_{1.3}$ compounds, the increase in ordering temperature is only from about 418 to 455 K.

The proposed model of antiferromagnetically coupled Fe sheets provides a rather straightforward explanation of the experimental results. The calculations presented in both this section and Sec. IV show that the magnetization curves are well reproduced. However, the model provides no explanation for the zero-field magnetization. A possibility mentioned by Coey et al.[4] is the appearance of stacking faults in the form of extra planes of Fe atoms. It is also possible that a slightly canted structure or impurities cause the spontaneous magnetization. Neutron-diffraction experiments are necessary to provide a definite answer on the spin structure.

VI. CONCLUSIONS

It is shown that all Nd$_6$Fe$_{13}M$ compounds with $M=$Au, Ag, Cu, Si, and Ga order antiferromagnetically around 415 K and that the, frequently reported, increase in magnetization at lower temperature is due to Nd$_2$Fe$_{17}$ impurity. Fields of 35 T are not enough to break the antiferromagnetic alignment between Dy and Fe moments. The R-Fe coupling $n_{R\text{Fe}}$ is of "normal" strength and sign for the $8f$ site and maybe for the

16*l* site too. The almost compensated magnetization at zero field in the heavy-*R*-substituted compounds indicates that the moments at both *R* sites have zero net magnetization. Hysteresis in the field dependence of the magnetization in La$_6$Fe$_{11}$Al$_3$ shows a significant Fe anisotropy to be present. A spin structure with ferromagnetic Fe sheets mutually antiferromagnetically coupled is proposed to explain the experimental results. A model for calculating the minimum energy in a free powder consisting of two sublattices has been extended to the calculation of the local energy minimum. This leads to magnetization curves with hysteresis due to the magnetocrystalline anisotropy. The magnetization behavior of La$_6$Fe$_{11}$Al$_3$ can be excellently reproduced. The more complicated behavior of the compounds with magnetic *R* ions can also be well understood within the two-sublattice model. The hydrides are all ferromagnetic (light-*R*) or ferrimagnetic (heavy-*R*) with ordering temperatures near 450 K, whereas the *R* ions have a reduced moment due to the hydrogen absorption. It is shown that within the proposed interaction scheme the Curie temperature of the hydrides must be approximately equal to the Néel temperature of the parent compounds.

[1] O. M. Sichevich, R. V. Lapunova, A. N. Soboley, Yu. N. Grin, and Ya. P. Yarmulek, Sov. Phys. Crystallogr. **30**, 627 (1985).

[2] J. Allemand, A. Letant, J. M. Moreau, J. P. Nozieres, and R. Perrier de la Bâthie, J. Less-Common Met. **166**, 73 (1990).

[3] P. Schrey and M. Velicescu, J. Magn. Magn. Mater. **101**, 417 (1991).

[4] J. M. D. Coey, Q. Qi, K. G. Knoch, A. Leithe-Jasper, and P. Rogl, J. Magn. Magn. Mater. **129**, 87 (1994).

[5] F. Weitzer, A. Leithe-Jasper, P. Rogl, K. Hiebl, A. Rainbacher, G. Wiesinger, W. Steiner, J. Friedl, and F. E. Wagner, J. Appl. Phys. **75**, 7745 (1994).

[6] Q. W. Yan, P. L. Zhang, X. D. Sun, B. P. Hu, Y. Z. Wang, X. L. Rao, G. C. Liu, C. Gou, D. F. Chen, and Y. F. Cheng, J. Phys.: Condens. Matter **6**, 3101 (1994).

[7] C. H. de Groot, F. R. de Boer, K. H. J. Buschow, D. Hautot, G. J. Long, and F. Grandjean, J. Alloys Compd. **233**, 161 (1996).

[8] T. Kajitani, K. Nagayama, and T. Umeda, J. Magn. Magn. Mater. **117**, 379 (1992).

[9] B-P. Hu, J. M. D. Coey, H. Clesnar, and P. Rogl, J. Magn. Magn. Mater. **117**, 225 (1992).

[10] Z. G. Zhao, C. H. de Groot, F. R. de Boer, and K. H. J. Buschow, Physica B **211**, 102 (1995).

[11] M. Rosenberg, R. J. Zhou, M. Velicescu, P. Schrey, and G. Filoti, J. Appl. Phys. **75**, 6586 (1994).

[12] B. Grieb and E.-Th. Henig, Z. Metallkd. **82**, 560 (1991).

[13] C. Müller, B. Reinsch, and G. Petzow, Z. Metallkd. **83**, 845 (1992).

[14] H. Peisl, in *Hydrogen in Metals*, Vol. 28 of *Topics in Applied Physics* (Springer, Berlin, 1978), Chap. 3.

[15] A. Leithe-Jasper, R. Skomski, Q. Qi, J. M. D. Coey, F. Weitzer, and P. Rogl, J. Phys.: Condens. Matter **8**, 3453 (1996).

[16] R. Gersdorf, F. R. de Boer, J. Wolfrat, F. A. Muller, and L. W. Roeland, in *High-Field Magnetism*, edited by M. Date (North-Holland, Amsterdam, 1983), p. 277.

[17] J. J. M. Franse and R. J. Radwański, in *Handbook of Magnetic Materials*, edited by K. H. J. Buschow (North-Holland, Amsterdam, 1993), Vol. 7, Chap. 5.

[18] R. van Mens, J. Magn. Magn. Mater. **61**, 24 (1986).

[19] M. Morariu, M. S. Rogalski, N. Plugaru, M. Valeanu, and D. P. Lazar, Solid State Commun. **92**, 889 (1994).

[20] D. Hautot, G. J. Long, F. Grandjean, C. H. de Groot, and K. H. J. Buschow, J. Appl. Phys. **81**, 5435 (1997).

[21] H. M. van Noort, D. B. Mooy, and K. H. J. Buschow, J. Appl. Phys. **57**, 5414 (1985).

[22] S. Jonen and H. R. Rechenberg, in *Magnetic Anisotropy and Coercivity in Rare-Earth Transition Metal Alloys*, edited by F. P. Missell (World Scientific, Singapore, 1996), Vol. 2, p. 200.

[23] H-S. Li, B-P. Hu, J. M. Cadogan, J. M. D. Coey, and J. P. Gavigan, J. Appl. Phys. **67**, 4841 (1990).

[24] T. T. M. Palstra, G. J. Nieuwenhuys, J. A. Mydosh, and K. H. J. Buschow, Phys. Rev. B **31**, 4622 (1985).

[25] I. A. Campbell, J. Phys. F **1**, L47 (1972).

[26] Z. G. Zhao, F. R. de Boer, V. H. M. Duijn, K. H. J. Buschow, and Y. C. Chuang, J. Appl. Phys. **75**, 7117 (1994).

[27] *Atlas of Crystal Structure Types*, edited by J. L. C. Daams, P. Villars, and J. H. N. Vucht (ASM International, Ohio, 1991).

[28] V. A. Yartys, O. Gutfleisch, V. V. Panasyuk, and I. R. Harris, J. Alloys Compd. **253**, 128 (1997).

[29] Z. G. Zhao, P. F. de Châtel, F. R. de Boer, and K. H. J. Buschow, J. Appl. Phys. **73**, 6522 (1993).

[30] Z. G. Zhao, X. Li, J. H. V. J. Brabers, P. F. de Châtel, F. R. de Boer, and K. H. J. Buschow, J. Magn. Magn. Mater. **123**, 74 (1993).

[31] A. Szytula, in *Handbook of Magnetic Materials*, edited by K. H. J. Buschow (North-Holland, Amsterdam, 1991), Vol. 5, Chap. 3.

[32] J. H. V. J. Brabers, V. H. M. Duijn, F. R. de Boer, and K. H. J. Buschow, J. Alloys Compd. **198**, 127 (1993).

[33] O. Oleksyn, P. Schobinger-Papamantellos, J. Rodríguez-Carvajal, E. Brück, and K. H. J. Buschow, J. Alloys Compd. **257**, 36 (1997).

[34] L. Néel, Nuovo Cimento Suppl. **6**, 1942 (1957).